www.ebscohost.com
www.gi.sanu.ac.rs, www.doiserbia.nb.rs,
J. Geogr. Inst. Cvijic. 67(2) (115–133)

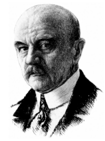

Original scientific paper

UDC:911.2:551.55(497.113)“2014”
DOI: https://doi.org/10.2298/IJGI1702115M

ANALYSIS OF A NON-SUPERCELL TORNADO IN SOMBOR ON JULY 10, 2014

*Jovan Mihajlović**[1]
* Polytechnic School, Kragujevac, Serbia

Received: June 30, 2017; Reviewed: July 20, 2017; Accepted: July 31, 2017

Abstract: Around 14:00 UTC, on July 10, 2014 a non-supercell tornado-a landspout, formed and occurred within a convective cloudiness in the S-SW upper air flow and moved over Sombor (45°46' N, 19°06' E, h=89 m). Synoptic conditions, type of synoptic situation which caused the landspout event, CAPE, LI indices and adiabatic stability of the atmosphere have been analysed in this paper. An analysis of sounding measurements and satellite images has also been done. Based on field survey analysis and using the Fujita scale method (*F*-scale), damage estimates have been shown in order to determine the tornado strength. The three main objectives of this research are: 1) analysis of atmospheric synoptic conditions that caused the landspout development in northern Backa using the data obtained from upper air and surface maps; 2) investigation into the satellite images data and radiosounding measurements; 3) to determine the evolution of the parent cloud from which the landspout developed using these methods. This article therefore represents a contribution to understanding of atmospheric conditions which favour a suitable synoptic and thermodynamic environment for a landspout genesis and development.

Key words: landspout, non-supercell tornado, synoptic types, cumulonimbus (Cb), Sombor

Introduction

A landspout or a waterspout over land belongs to local storms and it is a colloquial term for tornadoes developing from the parent cloud in the growing stages (Tcu) and the vorticity is connected with atmospheric boundary layer-ABL (Vujević, 1948; AMS, 2012). The term “*landspout”* was first introduced by Bluestein (1985) in the 1980s. It is an example of a non-supercell tornado since the parent cloud does not contain a strong mid-level mesocyclone and therefore is not connected with an organized rotation within the storm (AMS, 2012; Roberts & Wilson, 1995; Brady & Szoke, 1988; Brady & Szoke, 1989; Wilson & Wakimoto, 1989). A landspout is not visually connected with a wall cloud or a mesocyclone on the radar.

[1] Correspondence to: millennijum@hotmail.com

Vasiloff (1993) described the $F2$ landspout, while Fujita (1981) claims landspouts may even reach $F3$ strength. They are similar to Florida waterspouts and typical for Colorado (the so-called Denver Convergence Vorticity Zone-DCVZ) (Lee & Wilhelmson, 1997), but they have also been observed in Southern Ontario (Sills & King, 2000). Landspouts are frequent over the High Plains because of a dry surrounding which creates suitable synoptic and mesoscale preconditions. They may also occur in North Arkansas (Smith, 1996; Rogash, 1990).

Coriolis force may be irrelevant if the horizontal scale of atmospheric disturbance is sufficiently small, compared to the pressure gradient force (PGF) and centrifugal force. The force balance vertical to flow direction develops in cyclostrophic balance:

$$\frac{V^2}{R} = -\frac{\partial \Phi}{\partial n}, \tag{1}$$

and the cyclostrophic wind speed will be obtained if the equation (1) is solved by V:

$$V = \left(-R\frac{\partial \Phi}{\partial n} \right)^{1/2} \tag{2}$$

Pressure gradient force is always directed towards the curve centre, and centrifugal force from the curve centre, but cyclostrophic flow may be cyclonic and anticyclonic. Unless the isobars are straight, but are formed in a circular or irregular shape around the low pressure centre, as it is the case with a landspout, then the air flows along curved paths. In that case, the effect of centrifugal force is evident. If the motion becomes stationary, centrifugal force and deviatory force of the Earth rotation, together with the gradient force maintain the balance. The gradient wind equation, that is, the motion equation, has the following form (Vujević, 1948):

$$2\omega v \sin \varphi \pm \frac{v^2}{r} = -\frac{1}{\rho} - \frac{\Delta p}{\Delta D}, \tag{3}$$

since in the low pressure field, the pressure gradient force is directed towards the centre, while the deviatory force of the Earth rotation and centrifugal force are directed outward.

According to the conclusions drawn by Agee and Jones (2008) in their study of the tornado taxonomy, a landspout has been classified into type III (localized convective vortices and shear vortices) — IIIa. Agee and Jones (2008) described the type IIIa as a mesocyclone in ABL which develops under the influence of an intensive localized updraft which converges and stretches vertical vorticity.

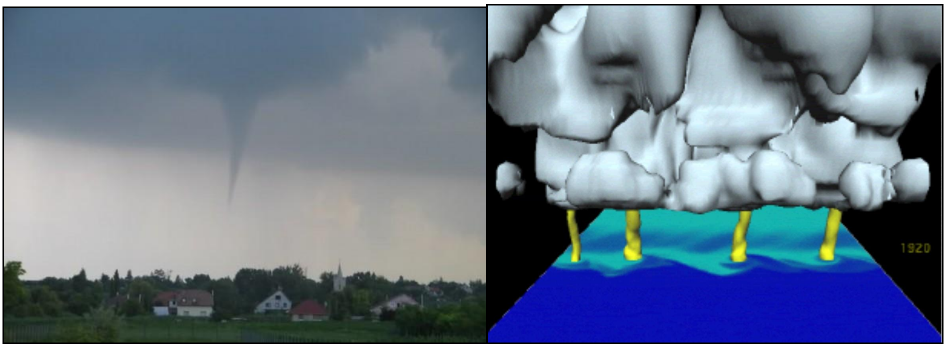

Figure 1. Landspout in Sombor, July 10, 2014 (left) (Source:Dnevne.rs (2014) and numerical model of non-mesocyclonic tornado (Lee & Wilhelmson, 1997) (right)

Around 14:00 UTC, on July 10, 2014, a non-supercell tornado — a landspout formed within a convective cloudiness which was moving over Sombor (φ 45°46' N, λ 19°06' E, h=89 m) in the S–SW upper air flow (Figure 1). This paper analyzes synoptic conditions and types of synoptic situations which caused the landspout to form, then CAPE and LI indices, as well as adiabatic stability of the atmosphere. An analysis of sounding measurements and satellite images has also been made. Based on field survey analysis, damage estimates have been shown in order to determine the tornado strength on the Fujita scale (*F*-scale). Main objectives in this research are: 1) analysis of atmospheric synoptic conditions which led to the landspout development in North Backa based on the data obtained from upper air maps and from the surface meteorological stations; 2) analysis of satellite images and radiosounding measurements; 3) analysis of the parent cloud evolution the landspout developed from. This paper makes contribution to understanding which atmospheric conditions create a favourable synoptic and thermodynamic environment for a landspout genesis and development in contrast to the paper which analyzed the same landspout event but using the radar analysis method (Mihajlovic, Ducić, Burić, & Ristić, 2015). Previous investigations on the territory of Serbia and surrounding area have been taken into consideration in this analysis (Maksimović, 1987; Ducić & Tanasijević, 1993; Radovanović, 2009; Mihajlović, Ducić, Burić, Ivanović, & Ristić, 2013; Mihajlović, Ducić, & Burić, 2014; Mihajlović et al., 2015; Mihajlović, Ducić, & Burić, 2016).

Data and methodology

During the research, archived data about surface and upper air (AT 500 mb) atmospheric structure, as well as synoptic diagrams for ML CAPE and LI, available on the http://www1.wetter3.de/ have been used. Sounding and wind hodograph have been done by the web application on the http://62.202.7.134/hpbo/sounding_create.aspx. Various products of satellite images from geostationary satellite — METEOSAT, available on the web page — http://www.eumetrain.org, have been used.

Based on the landspout research in Colorado and Oklahoma (Brady & Szoke, 1989; Bluestein, 1985), as well as in Ontario (Hogue, Joe, & Nichols, 1989; King, Leduc & Murphy, 1996; Murphy, 1991; Sills, 1998), a similar methodology has been applied during the landspout research in Sombor:

– method of synoptic analysis — analysis of surface and upper air (AT 500 mb) maps in main synoptic hours (00, 06, 12 and 18 UTC); according to absolute topography maps AT 500 mb, weather synoptic type has been determined;
– method of synoptic types — it has been determined according to the circulation on isobaric surface of 500 mb, as well as the position and orientation of the troughs and ridges which are related to the surface features. This method can be used both in temperate zones and in the Mediterranean region. There are four basic synoptic types: south-west flow (SW), long-wave trough (LW), short-wave trough (SWT) and closed low (CLOSED) (Sioutas, 2011; Sioutas and Flocas, 2003);
– method of CAPE and LI indices analysis — the two most important instability parameters have been analysed on complex synoptic maps from 12 to 18 UTC; a graphic representation of CAPE movement flow has been shown, a day before and after the storm;
– method of radiosounding analysis and wind hodograph-thermodynamic skew-T diagram (12 UTC) has been analyzed in details, and parameters indicating a non-supercell tornado event have been investigated; a wind hodograph has been investigated in a similar way;
– method of atmospheric stability analysis — atmosphere has been adiabatically investigated according to the sounding data, vertically on all levels;
– method of satellite image analysis — by using various products of geostationary weather satellite METEOSAT, an analysis has been

carried out making it possible to have a view “from the top“ on the storm;
– Fujita scale method-based on field analysis survey after the storm, the damage has been estimated by the Fujita scale (*F*-scale).

ESTOFEX (European Storms Forecast Experiment, http://www.estofex.org) (Figure 2) issued a storm forecast valid for the period from July 10, 2014, 06:00 UTC to July, 11, 2014, 06:00 UTC. Level 1 warning was issued for Romania and its surrounding area, forecasting mainly large hail, tornadoes, strong wind gusts and excessive rainfall. Level 1 warning was also issued for the Adriatic region, mainly because of large hail and excessive rainfall. Probability of lightning within 40 km in those regions was 50%.

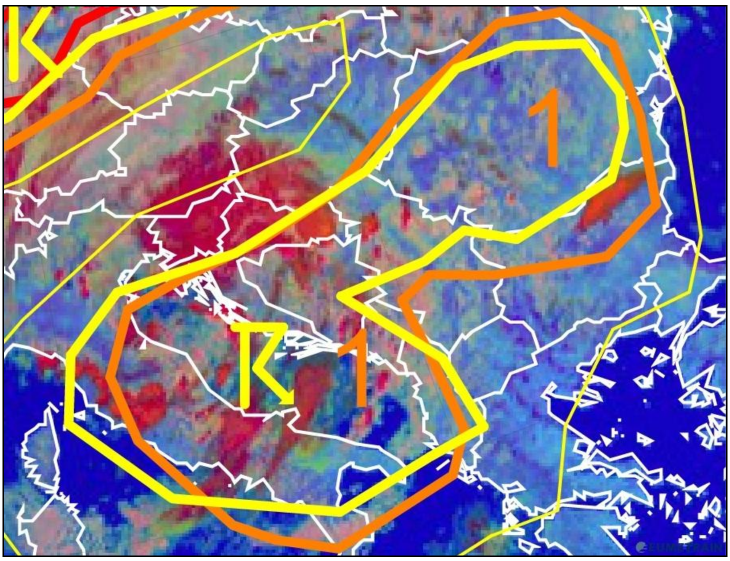

Figure 2. Day Microphysics RGB+ESTOFEX forecast, July 10, 2014 (http://www.eumetrain.org)

European Severe Weather Database (ESWD, http://www.eswd.eu), July 10, 2014 for the region of Sombor (φ 45°46' N, λ 19°06' E), recorded a strong wind.

Severe storm, followed by a large cumulonimbus (Cb) cloud of a high intensity, moved over Sombor (φ 45°46' N, λ 19°06' E, h=89 m) and surrounding area in the period from 14:00 to 14:30 UTC, within the upper air S–SW flow (Figure 3).

Synoptic situation — Synoptic type: CLOSED–SW

Surface synoptic situation over Europe on July 10, 2014 was a complex one with a few baric formations and frontal systems (Figure 4–left).

On the west, in the central part of the Atlantic, between the 40th and 50th parallel, an extensive ridge formed within which small anticyclonic centres developed. Within this ridge, a smaller one was formed in the form of a short wave, stretching over Ireland and the British Isles to the Norwegian Sea where a high pressure centre developed in the front part of the ridge. North from this high pressure system, an occluded cyclone in the fourth stage with corresponding frontal systems moved towards Iceland. On the eastern part of the cyclone and north from the British Isles, Ireland and Iceland, an occluded frontal disturbance with corresponding low pressure centres was noticed. The pressure in the extensive ridge axis was rising and, during the day, the ridge extended in the form of a long wave over the Bay of Biscay, Pyrenees, Western Mediterranean and the Gulf of Sidra. Within the ridge axis, small cyclonic and anticyclonic fields were formed all over the Mediterranean and North Africa.

A vast anticyclone with the centre over the Kola Peninsula developed in the east, closed by an isobar of 1,025 mb. A smaller anticyclonic centre was observed over Oslo and a high pressure centre developed within the shortwave ridge over Ukraine. There was a frontal disturbance around the system with corresponding warm and cold sectors. As the anticyclonic centre was moving southward, the frontal system became quasi-stationary.

Between these two high pressure systems a long frontal disturbance extended from the Svalbard and over Norway, the North Sea, Benelux, Germany and Poland. Warm and cold sectors were visible in this frontal system as well as cyclonic fields and vortices. The system was mostly a quasi stationary front with warm air streaming from the northeast, and cold air streaming from the southwest direction. It means that there was a strong temperature gradient at the surface and along this frontal disturbance. If it had stopped and deformed around an orographic obstacle, pressure gradient would have increased and there would have been conditions for stationary instability, which may have created favourable conditions for a convective potential.

The southern part of this long system was deformed because of the impact of the Alps and Central Europe block mountains; therefore, it slowed down and became stationary. At 00 UTC, a cyclonic field over Poland developed and the cold sector of this front stopped in front of the Carpathians and a convergence line was formed on the east of Romania and in Moldavia.

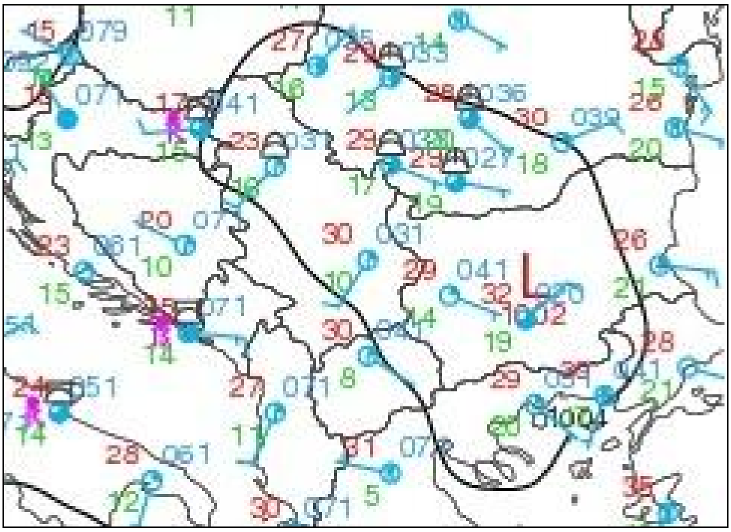

Figure 3. Enlarged SYNOP, July 10, 2014 at 14 UTC
(http://meteocentre.com/archive/archive.php?lang=fr)

From 12 UTC to 18 UTC, over the Apennine Peninsula, Adriatic Sea and Balkan Peninsula, several cyclonic fields and cyclonic centres developed at the surface, which were part of a large and deep upper level cyclone with the centre over the Balkan Peninsula and the Adriatic. South from these fields there was a high pressure ridge. As there was a strong surface warm air stream coming from the northeast direction, a warm sector of the frontal disturbance was developed over the eastern part of Serbia. Because of the cold air stream from the southwest direction in one section of this frontal disturbance, and a warm one coming from northeast direction, a convergence line was formed in Poland and Germany.

The landspout event which occurred in Sombor that day was most probably caused by a low pressure cyclonic vortex at the surface.

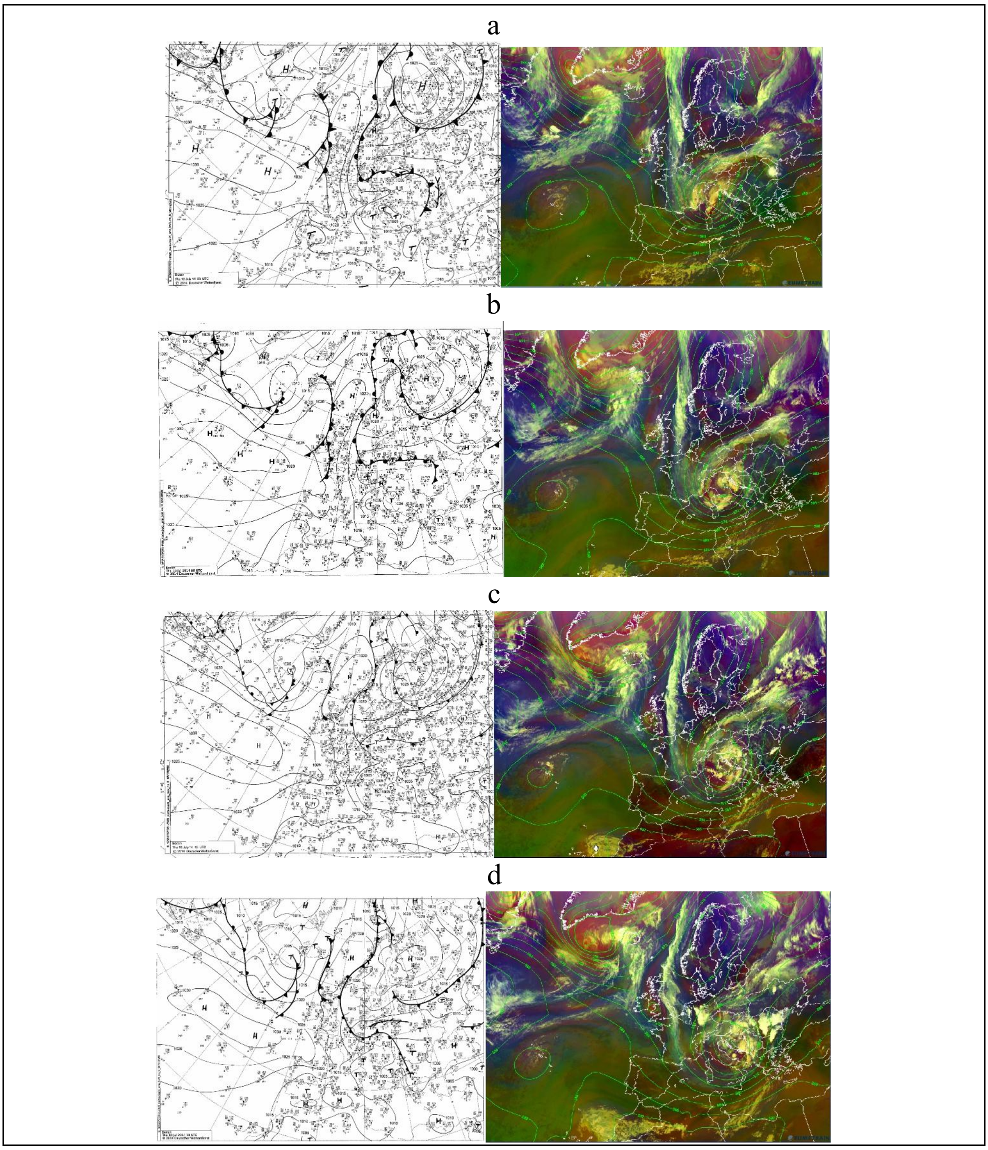

Figure 4. Surface level map (left) and Airmass RGB+H500 with corresponding cloudiness and atmospheric physics (right) at 00 UTC (a), 06 UTC (b), 12 UTC (c), 18 UTC (d), July 10, 2014 over Europe (http://www1.wetter3.de/; http://www.eumetrain.org)

On the absolute topography map AT 500 mb (Figure 4–right), on July 10, 2014, a vast shallow upper level trough in the form of a long wave was observed and a closed extensive upper level cyclone with the centre over the Gulf of Genoa was formed at the end of the trough at 00 UTC. Low geopotential values in the very centre of the cyclone show that there was a cold air intrusion in the upper atmosphere which contributed to the deepening of this vorticity system of closed isobars. This upper level cyclone then moved meridionally, from west to east, with the centre moving over the Adriatic and the Balkan Peninsula. This cyclone deepened under the influence of the cold air coming from the trough. In the upper atmosphere, above the observed area, there was a SW flow in the front part of the cyclone and in the front side of the trough which brought moist and unstable air.

Synoptic situation for July 10, 2014 was classified as CLOSED–SW. Over the Balkan Peninsula, Croatia and Slovenia there was an area of closed isobars, which indicated the presence of a vorticity system, that is, a cyclone at 500 hPa. Isolated low pressure centres were present at the surface. SW flow developed and a low pressure field was present with corresponding frontal systems.

Such synoptic environment created favourable atmospheric conditions for convective instability and a landspout development. Warm and dry air coming from northeast was present at the surface, while in the upper atmosphere there was moist and cold air coming from southwest. Local cyclonic field was also formed at the surface. Thermodynamic conditions on synoptic scales created ideal conditions for a landspout event in Sombor.

CAPE and LI analysis

CAPE is available energy that a storm can use for its development and it comes from released energy during the process of condensation. CAPE is an important indicator of the updrafts in a thunderstorm. It is a positive area on the “skew-T” diagram. Theoretically, it is a region where the temperature of an air parcel is higher than the temperature of the environment. The speed of updrafts is related to the CAPE (http://www.theweatherprediction.com/habyhints/305/). The Lifted index (LI) help to estimate the instability of the low level parcel in the troposphere. The higher negative value of the LI, the more instable atmospheric boundary layer is (http://www.theweatherprediction.com/habyhints/300/).

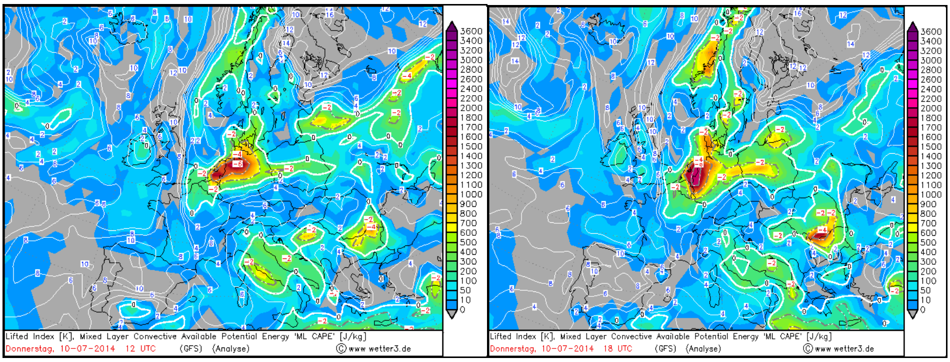

Figure 5. Lifted index (LI) (lines) and 'ML CAPE' (colours), July 10, 2014 at 12 UTC (left) and at 18 UTC (right) over Europe (http://www1.wetter3.de/)

At 12 UTC, just before the thunderstorm developed in Sombor, positive CAPE with the $1100\ J\ kg^{-1}$ core was observed on a wide area of Backa, Baranja, Slavonia and Srem, which represented an indicative and sufficient quantity of energy for severe weather development (Figure 5). At 18 UTC, after the thunderstorm passed, this positive CAPE area decreased at about $500\ J\ kg^{-1}$ (Figure 6).

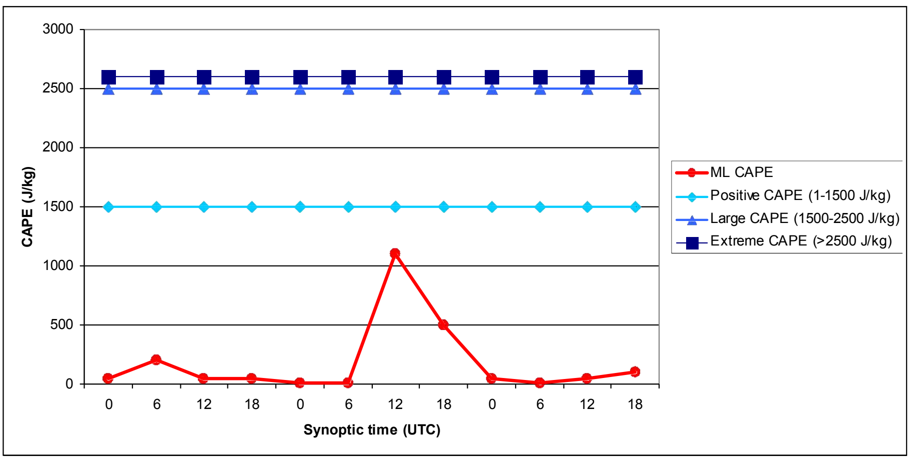

Figure 6. CAPE values (J/kg) in main synoptic hours (UTC)

Lifted index (LI) has the same values at 12 and 18 UTC and it is −2, which indicates marginal instability. Analysis of the both parameters points to the fact that there was sufficient instability energy in the atmosphere that day and that ABL was unstable, but not that much to cause a supercell and tornado development. The conclusion is that there were favourable atmospheric conditions for a landspout event (Figure 5).

Sounding and hodograph analysis

Sounding (skew-t) and wind hodograph (Figure 7) for Belgrade station (13275), July 10, 2014 at 12 UTC are shown.

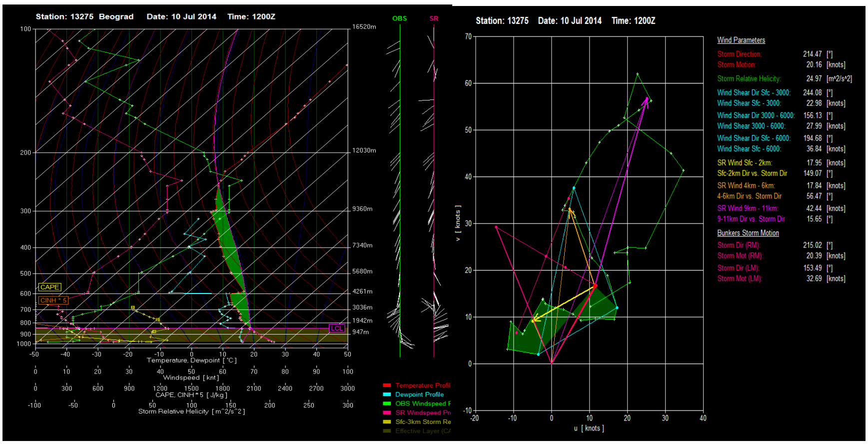

Figure 7. Sounding (skew-t) and wind hodograph for Belgrade, July 10, 2014 at 12 UTC (http://62.202.7.134/hpbo/sounding_create.aspx)

Vertical profile of the atmosphere points to adiabatic instability from the lowest layers (LCL AGL = 1,257 m), and, through the whole vertical profile, up to approximately 10,000 m (convective height is on 9.15 km). The surface temperature was over 20 °C (convective temperature is 25.16 °C), and dew point temperature was about 20 °C. The zero isotherm height was $H_0 = 3.3\ km$, and the height of isotherm $H_{-6} = 4.3\ km$. The temperature of the parcels adiabatically rising up was higher than the environmental temperature, therefore, there was a good buoyancy, while the temperature lapse rate in the 850–600 mb layer was 19.2 °C, which pointed to conditions for a convective initiation. Maximum hail size was estimated at about 4.3 cm.

Instability indices — $CAPE = 1109\ J\ kg^{-1}$ ($CAPE\ Virt. = 1242\ J\ kg^{-1}$) and LI = −3.53 °C, point to scattered and widely spread thunderstorms. UVV has been calculated from CAPE and amounts to 47 m s^{-1}, which points to a strong updraft. DCAPE (LFS = 665 mb) is $866\ J\ kg^{-1}$, and thus the energy of the clod downdrafts (DVV) is 27 m s^{-1}. Other convective indices (SI, MTI, TT, KO, and SWISS 12) pointed to expected widespread thunderstorms.

Observed wind profile indicates a strong directional and speed wind shear from the surface up to 200 mb. The greatest changes in speed and direction the wind made in the 600–800 mb layer, but then it suddenly increased the speed up to the 250 mb layer. The storm moved at the speed of 20 knots, and the storm relative wind had values of 18 knots (Sfc-2 km), 18 knots (4–6 km) and 42 knots (9–11 km), which points to the probability of a classic tornado supercell event. However, since the helicity, EHI, effective shear and 3 km vorticity generation potential were small; there were no supercells and tornadoes.

Analysis of satellite images

Following products of the second generation meteorological satellite METEOSAT have been used: Airmass RGB, Severe Storms RGB and Pseudo WV, on July 10, 2014 at 12 UTC. Satellite images indicate convective cloudiness over the north of Serbia (Srem and Banat), and its surroundings, which corresponds with the synoptic situation on that day.

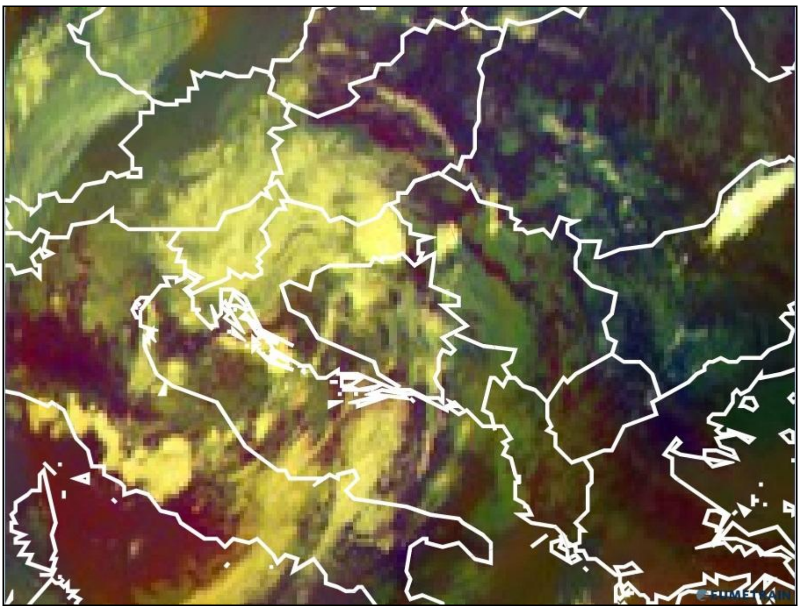

Figure 8. Airmass RGB, July 10, 2014 at 12 UTC (http://www.eumetrain.org)

The Figure 8 in Airmass RGB colour combination (12 UTC) shows a developing convective cell over Srem, shifting and spreading towards the north under the influence of S-SW upper air flow. The convective cell on the image can be recognized by the shape, not by colour. Red shades on the image point to the presence of warm dry air mass in the area of Banat and Backa, while the green shades indicate highly moist air mass in the upper troposphere, right behind the convective cloudiness. This upper level system was moving from the west towards the east, over the territory of Serbia.

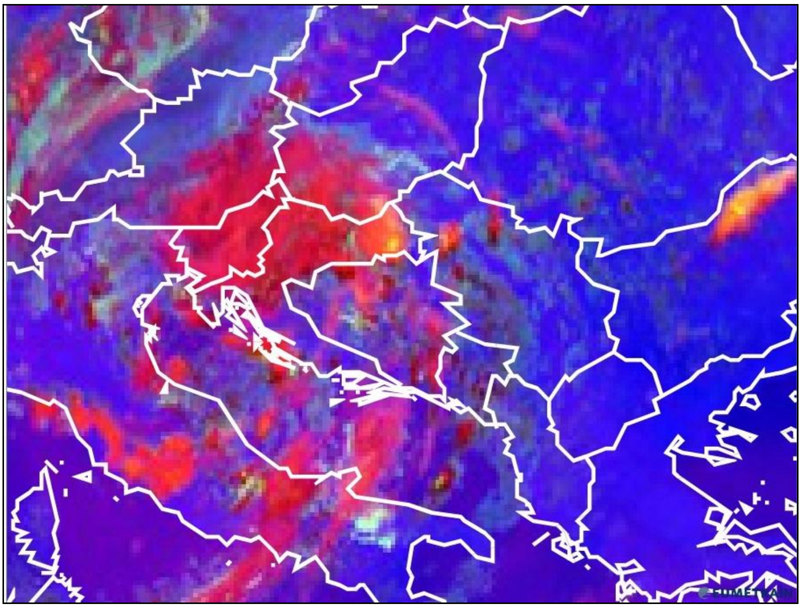

Figure 9. Severe Storms RGB, July 10, 2014 at 12 UTC (http://www.eumetrain.org)

The Figure 9 — Severe Storms RGB (12 UTC) — light yellow and orange colours point to an area of a rising updraft on the top of the convective cell. This is an active part of the thunderstorm system. The cloud tops are very cold and contain ice crystals. The image points to a strong convective cloud and its active parts.

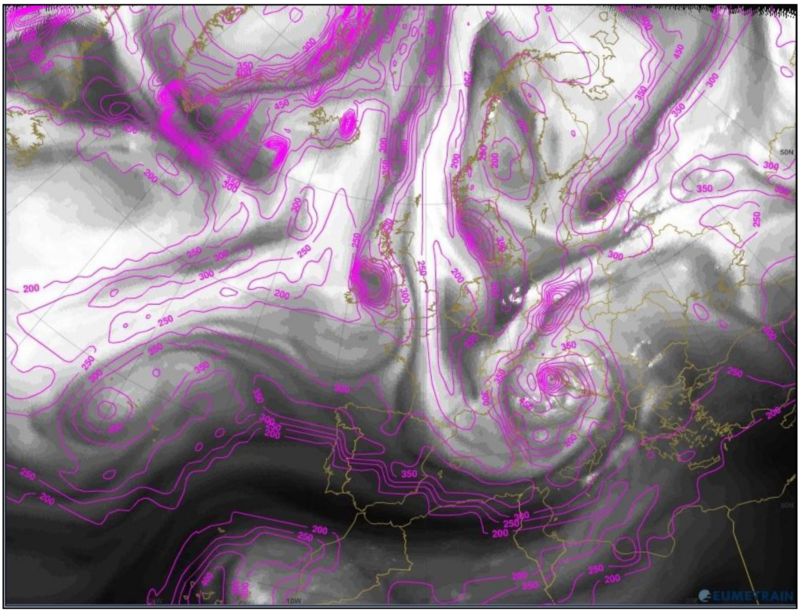

Figure 10. Pseudo WV+Height PV=1.5, July 10, 2014 at 12 UTC over Europe (http://www.eumetrain.org)

In the Figure 10 — WV 6.2 light-temperature, a vast upper level cyclone with the centre over the Gulf of Trieste can be seen, which corresponds with the synoptic conditions on that day. In the very centre of the cyclone, PV isobars are close spaced and are located on the height between 400 and 450 mb. Air mass which caused the landspout event in Sombor can be seen on the image, and the 350 mb isobar (with PV = 1.5) passes over it. It is thought that the thunderstorm cloud got vorticity from this upper level cyclone, that is, from the PV core in its centre.

Discussion and conclusion

A severe thunderstorm cloud which spread over the area of Sombor from 14–14:30 UTC (16–16:30 CET) on July 10, 2014, caused a strong thunderstorm weather and heavy rain, as well as a landspout. A convective cell, which was located within the convective cloudiness, moved towards the north under the influence of a dominant S–SW upper air flow.

There was warm and muggy weather over the territory of Serbia on July 10, 2014. The air temperature in the hottest part of the day in most parts of the country was 25 °C, and the southwest wind of moderate intensity was blowing.

In the early afternoon hours a convective cloudiness developed over the wide area of southwest and central Serbia and within a frontal disturbance which was moving towards the east and northeast in the SW upper air flow. Isolated convective cells were noticed in various parts of the country, some of them probably being supercells. The dominant SW upper air flow brought moist air to the upper troposphere which caused moisture to increase in the warm air mass around the frontal disturbance and thus perfect conditions for convective initiation and intensification were created. Thermal instability of the atmosphere favoured development of severe convective clouds (TCu/Cb)-CAPE was positive and was about 1,100 $J\ kg^{-1}$. Dynamic conditions were also satisfied, since the directional and speed wind shear was clearly noticed from the surface and mostly in the 600–800 mb layer. However, parameters indicating the quantity of rotation in the storm-helicity and EHI, did not predict a supercell and tornado. Convective events over the wide area of Banat were intensified in the period from 15:00–18:00 CET (13:00–16:00 UTC).

Synoptic analysis, instability parameter analysis, radiosounding, satellite analysis and atmospheric instability analysis were carried out. The results of the analyses pointed to thermal instability over a wide area of Sombor on that day, but also to favourable dynamic conditions on the surface and in the upper atmosphere.

Considering the landspout event in Sombor on July 10, 2014 we can say that there was a process in the atmosphere, as well as an increased instability energy (CAPE) and favourable dynamic conditions, which together caused local vorticity in the ABL shallow layer and concentrated source of vertical vorticity on the surface, which were, under the influence of intensive warm rising updrafts, stretched into a misocyclone–landspout. There was sufficient heat at the surface, but not in the upper atmosphere. The core of the upper level cyclone was supplied by the cold air from the north, so that the cold air in upper layers additionally destabilized the atmosphere.

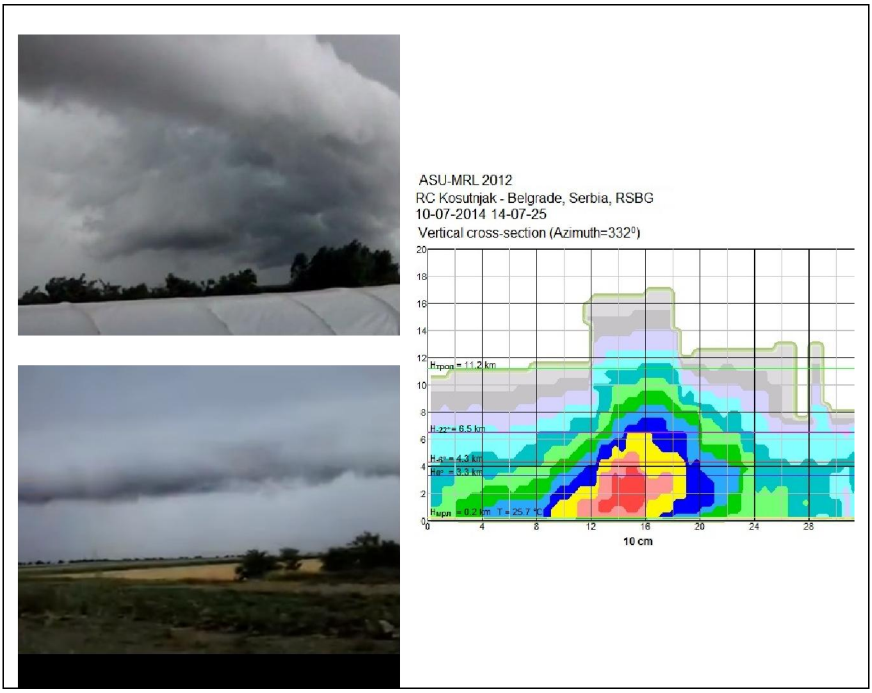

Figure 11. Cloudiness (Cb arcus) which accompanied the severe weather in Sombor (https://www.youtube.com/watch?v=ESelJsBpCS) and the corresponding radar image-vertical cross-section (Azimuth=332^0) (10 cm), on July 10, 2014 at 14:19 UTC (http://www.hidmet.gov.rs)

Since it is impossible to have direct measures of the wind speed in a landspout, Fujita scale method (*F*-scale) was used in order to determine an approximate wind speed. The landspout came from the west, uprooted trees and fruit trees, carried away fences, building material, roofs and bicycles. It was accompanied by a loud hissing sound, stormy wind, and a cloudburst. There were no injured people, but the damage was considerable. Applying the Fujita scale method and based on radar criteria, it can be concluded that the landspout which swept over Sombor on July 10, 2014 (Figure 11) caused minor damage and therefore belongs to F0 category of landspouts (from 18–33 m s^{-1} on *F*-scale).

Acknowledgements

I would like to express my sincere gratitude to PhD Vladan Ducic who has helped me in realization of this paper and to PhD Dragan Buric who gave me helpful suggestions.

References

Agee, E., & Jones, E. (2009). Proposed Conceptual Taxonomy for Proper Identification and Classification of Tornado Events, *Weather and Forecasting*, *24,* 609–617, doi: https://doi.org/10.1175/2008WAF2222163.1.

AMS Glossary — American Meteorological Society (2012). Retrieved on September 17, 2016, from http://glossary.ametsoc.org/wiki/Landspout

Bluestein, H. B. (1985). The formation of a "lands-pout" in a "broken-line" squall line in Oklahoma. *Preprints, Fourteenth Conference on Severe Local Storms* (pp. 267–270). Indianapolis, IN: American Meteorological Society.

Brady, R. H., & Szoke, E. J. (1988). The landspout — a common type of northeast Colorado tornado. *Preprints, Fifteenth Conference on Severe Local Storms* (pp. 312–315). Baltimore, MD, Boston MA: American Meteorological Society.

Dnevne.rs (2014). Retrieved on October 16, 2014, from http://www.dnevne.rs/zuta-stampa/nevreme-u-somboru-vazdusna-pijavica-cupala-drvece-rusila-krovove

Ducić, V. & Tanasijević, Z. (1993). Pojava trombe u valjevskom kraju. *Glasnik Srpskog geografskog društva, 73*(1), 25–32. Retrieved from http://www.digitalna.nb.rs/wb/NBS/casopisi_pretrazivi_po_datumu/glasnik_srpskog_geografskog_drustva/1993/b073#page/9/mode/1up

EUMeTrain (n.d.). Retrieved on September 17, 2016, from http://www.eumetrain.org

European Severe Weather Database (n.d.). Retrieved on September 12, 2016, from http://www.eswd.eu

European Storm Forecast Experiment @ estofex.org (n.d.). Retrieved on September 12, 2016, from http://www.estofex.org

Fujita, T. T. (1981). Tornadoes and downbursts in the context of generalized planetary scales. *Journal of Atmopheric. Science, 38,* 1511–1534. doi: https://doi.org/10.1175/1520-0469(1981)038<1511:TADITC>2.0.CO;2

Haby Hints — The Weather Prediction (n.d.). Retrieved on September 12, 2016, from http://www.theweatherprediction.com

Hogue, R., Joe P., & Nichols, T. R. (1989). The 17 September 1988 weak tornadic storm in Metro Toronto, Ontario Region. *Atmospheric Environment Service, 17, Technical Note. 89–2*.

King, P., Leduc M. J., & Murphy, B. P. (1996). The climatology of tornadoes in southern Ontario: Possible effects of lake breezes. *Preprints, Eighteenth Conference on Severe Local Storms* (pp. 627–630). San Francisco, CA: American Meteorological Society.

Lee, B. D., & Wilhelmson, R. B. (1997). The numerical simulation of non-supercell tornadogenesis. Part I: initiation and evolution of pretornadic misocyclone circulations along a dry outflow boundary, *Journal of the Atmospheric. Sciences., 54*, 32–60. doi: https://doi.org/10.1175/1520-0469(1997)054<0032:TNSONS>2.0.CO;2

Maksimović, S. (1987). Mesto i uloga meteorologije u zaštiti od elementarnih nepogoda*,* U: *Zbornik radova „Prvo jugoslovensko savetovanje o elementarnim nepogodama i katastrofama"*(pp. 221 – 232). Beograd: Savezni hidrometeorološki zavod,

MétéoCentre.com (1995–2016). Retrieved on September 12, 2016, from http://meteocentre.com

Mihajlović, J., Ducić, V., Burić, D., Ivanović, R., & Ristić, D. (2013). Landspout across Novi Beograd, 24 may 2012: Synoptic analysis. *Glasnik Srpskog geografskog društva*, *93*(2), 55–72. doi: https://doi.org/10.2298/GSGD1302055M

Mihajlović, J., Ducić, V., & Burić, D. (2014). Tornado occurrence nearby Valjevo on 27 May 2014 – analysis of weather situation, *Journal of the Geographical Institute Jovan Cvijić SASA, 64*(3), 279–292. doi: https://doi.org/10.2298/IJGI1403279M

Mihajlović, J., Ducić, V., Burić, D., Ristić, D. (2015). Tromba u Somboru — analiza slučaja 10.07.2014. Zbornik radova, *4. Srpski kongres geografa sa međunarodnim učešćem „Dostignuća, aktuelnosti i izazovi geografske nauke i prakse", povodom 150 godina rođenja Jovana Cvijića.* Kopaonik 07–09.10.2015, Univerzitet u Beogradu, Geografski fakultet, Srpsko geografsko društvo.

Mihajlović, J., Ducić, V., & Burić, D. (2016). Tornadic waterspout event in Split (Croatia) – analysis of meteorological environment, *Journal of the Geographical Institute Jovan Cvijić SASA, 66*(2). doi: https://doi.org/ DOI:10.2298/IJGI1602185M

Murphy, B. P. (1991). Tornado and flash flood in southwestern Ontario on 31 May 1991. *Atmospheric Environment Service of Canada, Technical Note*. 91–3.

Republic Hydrometeorological Service of Serbia — RHMSS (2016). Retrieved on September 12, 2016, from http://www.hidmet.gov.rs

Radovanović, M. (2009). Tromba kod Inđije — analiza slučaja 06. juna 2008. godine. *Glasnik Srpskog geografskog društva, 89*(4), 295–304.

Roberts, R. D., & Wilson, J. W. (1995). The genesis of three nonsupercell tornadoes observed with dual-Doppler radar. *Monthly Weather Review, 123*, 3408–3436. doi: https://doi.org/10.1175/1520-0493(1995)123<3408:TGOTNT>2.0.CO;2

Rogash, J. A., (1990). *An investigation of forcing mechanisms during a surprise tornadic thunderstorm*, *NOAA Technical Memorandum, NWS SR-128*. Fort Worth, TX: Scientific Services Division. Retrieved from http://www.pmarshwx.com/research/srtm/sr-128.pdf

SevereWeather.ch — Create Sounding (n.d.). Retrieved on September 13, 2016, from http://62.202.7.134/hpbo/sounding_create.aspx

Sills, D.M.L. (1998): Lake and land breezes in southwestern Ontario: observations, analyses and numerical modelling (Doctoral dissertation). Retrieved from The Smithsonian/NASA Astrophysics Data System

Sills, D. M. L., & King, P. W. S. (2000). Landspouts at lake breeze fronts in southern Ontario. *Preprints, Twentieth Conference on Severe Local Storms* (pp. 243–246). Orlando, FL: American Meteorological Society

Sioutas, M. V. (2011). A tornado and waterspout climatology for Greece. *Atmospheric Research, 100*, 344–356. doi: https://doi.org/10.1016/j.atmosres.2010.08.011

Sioutas, M. & Flocas, H. A. (2003). Hailstorms in Northern Greece: synoptic patterns and thermodynamic environment. *Theoretical and Applied Climatoogy, 75*, 189–202. doi: https://doi.org/10.1007/s00704-003-0734-8

Smith, R. (1996). *Non-supercell tornadoes: A review for forecasters. Technical attachment.* Memphis, TN: NWSFO

Vasiloff, S.V. (1993). Single Doppler radar study of a variety of tornado types. In C. Church, D. Burgess, C. Doswell & R. Davies-Jone (Eds.), The *Tornado: Its Structure, Dynamics, Prediction, and Hazards* (pp. 223–231). American Geophysical. Union. doi: https://doi.org/10.1029/GM079p0223

Vujević, P. (1948). *Meteorologija.* Beograd: Prosveta

Wetter3-aktuelle Wetterkarten (n.d.). Retrieved on September 13, 2016, from http://www1.wetter3.de

Wilson, J.W., & Wakimoto, R.M. (1989). Non-supercell tornadoes. *Monthly Weather Review, 117*, 1113–1140. https://doi.org/10.1175/1520-0493(1989)117<1113:NST>2.0.CO;2

YouTube (2014). Retrieved on October 12, 2014, from https://www.youtube.com/watch?v=ESelJsBpCS